Asia-Pacific Journal of Science and Technology: Volume: 28. Issue: 03. Article ID.: APST-28-03-19. Research Article

APST

Asia-Pacific Journal of Science and Technology

https://www.tci-thaijo.org/index.php/APST/index

Published by the Research and Graduate Studies,
Khon Kaen University, Thailand

Kerf-width optimization and surface characterization of wire electric discharge machined Ti-6Al-4V using response surface method

Deepak Doreswamy[1], Sai D. Shreyas[1], Satheesh Javaregowda[2], Anjaiah Devineni[3] and Subraya K. Bhat[4,*]

[1]Department of Mechatronics, Manipal Institute of Technology, Manipal Academy of Higher Education, Karnataka, India
[2]Department of Mechanical Engineering, SJB Institute of Technology, Bangalore, India
[3]Department of Automobile Engineering, School of Automobile, Mechanical & Mechatronics Engineering, Manipal University, Jaipur, India
[4]Department of Mechanical and Industrial Engineering, Manipal Institute of Technology, Manipal Academy of Higher Education, Karnataka, India
[*]Corresponding author: sk.bhat@manipal.edu

Received 1 June 2022
Revised 17 June 2022
Accepted 26 June 2022

Abstract

Wire-Electric Discharge Machining (WEDM) is one of practicable advanced machining techniques for machining of hard materials such as Titanium alloys precisely. It is critical to optimize the settings for control parameters to achieve the desired levels of kerf width and dimensional tolerance. Considering this objective, this research investigates the effects of current, pulse on time (T_{on}) and pulse off time (T_{off}) on kerf width of Wire-Electric Discharge (WED) machined Ti-6Al-4V Titanium alloy. The study showed that, increase in current from 2 A to 6 A resulted in increase of kerf width by 9.34% and 12.62%, respectively. But increase of T_{off} from 20 µs to 30 µs led to a sharp reduction in kerf width by about 6.14%. Further, a regression model is developed to predict the surface roughness with coefficient of determination (R^2) =90.11%. The machined surfaces are characterised by the presence of voids and microcracks on the recast layers, formation of micro-globules, ridges and craters due to thermal effects. Within the range of study T_{off} showed significantly larger influence in minimizing the kerf width compared to other parameters of the study.

Keywords: Ti-6Al-4V, Kerf width, Wire-EDM, Pulse-on time, Pulse-off time, Peak current

1. Introduction

Ti-6Al-4V is one of the Titanium alloys which is an attractive choice across numerous applications including but not limited to automobile, petrochemical, aerospace, and biomedical engineering domains due to its superior mechanical strength, exceptional corrosion resistance, and its ability to maintain their properties at high temperatures [1]. However, these very same superior qualities create hurdles when it comes to its machining using traditional manufacturing techniques because of the large workpiece deflections, drastic cutting temperatures, and significant tool wear rates which are caused during their machining [2]. Additionally, the work hardening caused during their machining reaches severe levels causing extremely high machining forces and complications related to vibration, e.g., spring-back and chatter, thus making conventional machining techniques a difficult path to machine them into required dimensions [3]. Although, various non-conventional machining techniques have been explored for their machining, they have their own troubles associated with environmental safety during usage and disposal of chemicals and limitations of affordability [4]. Considering these challenges, Wire Electric Discharge Machining (WEDM) is a preferred method for machining of titanium alloys over other machining techniques [5-8].

WEDM involves the process of erosion of work material, wherein the workpiece to be machined is eroded by the utilization of thermal energy in the form of sparks which are produced by a conversion of form of energy from

electrical energy [9]. By generating recurrent and controlled amounts of sparks between an electrode (in the form of a wire) and the workpiece, the material erosion process is made possible. These sparks generate extreme temperatures reaching around 10,000˚C which is ample enough to evaporate or grind away the work material in a localized region causing material removal. The evaporated or eroded material at a minuscule level is flushed away from the workpiece surface by a stream of dielectric fluid medium flowing around the machined surface [9]. A series of control parameters (or process parameters) such as, pulse on time (T_{on}), pulse off time (T_{off}), wire speed, wire feed rate, wire tension, discharge current, voltage, dielectric flow rate etc., which can be varied during machining using WEDM for achieving the required levels of output characteristics [10,11]. T_{on} is the time duration during which spark discharge takes place, whereas pulse T_{off} is the duration of time of no discharge in between each time duration of T_{on} [9]. Wire speed, feed rate, and tension are related to the movement and fixturing of the cutting wire. The current and voltage measure the amount of power spent in discharge machining.

In light of these facts, it is essential to determine the optimized WEDM process parameters to arrive at the required machining performance characteristics. To this end, numerous techniques of optimization [12-19] have been employed to determine the optimum settings of WEDM process parameters during machining of Titanium alloys. Design of experiments approach has been utilized to analyze the effects of various process parameters on the output machining characteristics of Titanium alloys [20,21] Among the various techniques used, Response Surface Method (RSM) is one of the popularly used techniques in the optimization of WEDM of Titanium alloys [16-19]. The goal of RSM is to identify the optimum value of the control variables at which a particular operation can be accomplished while satisfying certain output characteristic criterion. One of the main advantages of RSM in comparison with other optimization techniques is its ability to produce a realistic combination of process parameter settings, which somehow is not achievable by other techniques where there is a possibility that the determined combination of process parameters is absent in the machine under consideration [16]. Therefore, this study utilizes RSM as the primary optimization technique.

Among various important topics of research in the field of WEDM of Titanium alloy Ti-6Al-4V, the choice of the electrode materials and the fluid media are one of equal importance, which have not received appropriate attention [6]. Regarding the electrode material, numerous materials including pure and coated forms of materials such as, aluminum, brass, copper, graphite, tungsten carbide, steel, etc., have been investigated in the WEDM of Titanium [22-24]. But in comparison to the above electrode materials, fewer studies have paid attention the suitability and performance of molybdenum wires as the electrode material, and their relationship with the variation of controlling parameters [25,26]. With regards to the effects of fluid dielectric media, oil and water have been explored, and by comparisons made between the two, oil has demonstrated lower stability characteristics and higher quantities of wear rates of electrode material as that exhibited by water [27]. Based on these assessments from past literature, the present study was carried out by selecting deionized water as the dielectric fluid and molybdenum as the electrode material, which needed to be investigated in more detail.

In terms of the output performance physical characteristics achieve during WEDM, the slot width (also called as kerf width), the material removal rate, and the surface roughness (SR), are the chief qualities which have garnered attention in the literature [28,29]. Further, specific consideration has been placed on the interrelationships between the individual control parameters such as, T_{on}, T_{off} and peak current and the resulting machining attributes such as, material removal rate and surface roughness [30]. With regard to the kerf width, researchers have investigated the optimum values of T_{on}, T_{off} and peak current [29,30]. In terms of peak current, typically, studies have chosen higher peak current values, such as, between 8 A - 12 A [29] and 170 A - 210 A [30]. But the WEDM machines can operate at even lower current settings of 2A - 6A, which has been adopted in the present study. Further, in terms of T_{on} and T_{off}, the range of their durations have been limited to between 110 μs - 118 μs [29] and 45 μs - 55 μs, respectively, which is again on the higher side [30]. In the present paper, these control parameters are also investigated for a wider range within their feasible values available in the WEDM machine. The findings of the present study thus aim to resolve the important research lacuna in terms of the operating range of the control parameter values which have received less attention in studies of WEDM of Ti-6Al-4V alloy available in the literature and therefore is an important contribution of the present paper.

Research available in literature has shown that WEDM has an incredible scope as a candidate for a suitable machining technique for machining of Titanium Ti-6Al-4V. Nevertheless, there is a further need to perform a kerf width minimization by optimizing the combinations of control parameters. Particularly, the present study uses a unique combination of electrode wire of 0.18 mm made up of molybdenum while utilizing deionized water as the dielectric fluid during WEDM of Ti-6Al-4V, with a distinctive range of the operating parameters, i.e., peak current, T_{on}, and T_{off} [31,32]. The present makes use of Analysis of Variance (ANOVA), regression modeling, and RSM to optimize the WEDM of Ti-6Al-4V by analyzing the effects of peak current, T_{on}, and T_{off} to obtain minimum kerf width (which is closely related to dimensional tolerance and surface finish obtained during machining). Furthermore, the micrographic morphological analysis of the machined surface is very much a necessity to evaluate the nature of the surface and dimensional tolerance which could be obtained by machining.

2. Materials and methods

2.1 Experimental setup

The automatic computer numerical control (CNC) WEDM machine, "Concord Versa Cut" consisting of a 320 mm × 400 mm table was utilized for performing the machining operations in this study (Figure 1). Initially, for the preparation of the samples, a whole plate of titanium is cut into pieces measuring 150 mm × 50 mm × 2 mm. For these work samples, machining is performed for each combination of selected control parameter for length of 10 mm each. Subsequent to the machining operations, the kerf width along each side is measured from the test samples (Figure 2). Table 1 presents the material composition results of the Ti-6Al-4V sample which were obtained by conducting X-ray Diffractometer (XRD) tests at Varsha Bullion Elemental Analab, Mumbai, India.

Figure 1 The experimental setup.

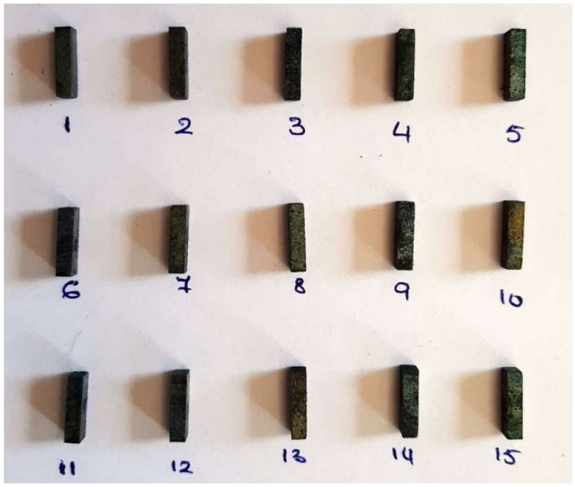

Figure 2 Wire-EDM machined test samples.

Table 1 Material composition of Ti-6Al-4V.

Chemical composition	Percentage
Ti	89.54
Al	5.60
V	4.50
Fe	0.23
C	0.01
Cr	0.03
Cu	0.09

2.2 Design of experiments (DOE)

As discussed in the introduction, WEDM consists of various controlling parameters which govern the output physical characteristics which may be obtained after the machining operations on a given work material. To select a few parameters for the investigation and to arrive at their suitable range of values, knowledge gained by previous studies by the authors [31,32] was made use of. Thus, based on the previous studies carried out by the authors, T_{on}, T_{off} and peak current were chosen as the key parameters which dictate the output performance characteristics. The effects of other operating parameters, such as, pertaining to the speed of the electrode wire and the tension applied on it, the composition of the dielectric fluid used to flush the eroded material and its pressure, voltage of electricity supplied to generate the sparks, etc., were fixed during all the machining trials which were performed. Table 2 presents the values of the fixed control parameters. The central composite design of the RSM was used to design the experimental trials (Table 3) and the experimental plan (Table 4).

Table 2 Parameters kept constant during the experiments.

Parameters	Values
Wire speed (m/s)	4.4 m/s
Wire tension (kg/f)	8 kg/f
Dielectric fluid	Deionized water + cleanser gel
Fluid pressure (dm^3/min)	40 dm^3/min
Servo Voltage (V)	80 V

Table 3 The range of Wire-EDM parameters chosen in the present study.

Parameters	Unit	Level 1	Level 2	Level 3
T_{off}	µs	10	20	30
T_{on}	µs	20	35	50
Current	A	2	4	6

Table 4 Coded experimental plan for the experimental trials using levels described in Table 2.

Run Order	Current (A)	T_{on} (µs)	T_{off} (µs)
1	Level 1	Level 1	Level 2
2	Level 2	Level 2	Level 2
3	Level 1	Level 3	Level 2
4	Level 3	Level 2	Level 1
5	Level 2	Level 1	Level 3
6	Level 3	Level 1	Level 2
7	Level 2	Level 3	Level 3
8	Level 1	Level 2	Level 3
9	Level 2	Level 2	Level 2
10	Level 3	Level 3	Level 2
11	Level 2	Level 2	Level 2
12	Level 1	Level 2	Level 1
13	Level 3	Level 2	Level 3
14	Level 2	Level 3	Level 1
15	Level 2	Level 1	Level 1

2.3 Kerf width measurement and morphological analysis

The slot width or kerf width is measured using optical microscope (Figure 3). Width was measured at three different locations along the length and the average of the measurements is considered for the analysis. A sampling length of 2.5 mm was used for recording the measurements, and typically, the measurements were made at the upper, middle, and lower regions of the cut kerf surface. Scanning electron microscope (Make: Zeiss) and Mitutoyo Inverted metallurgical microscope (Model: IM 7000) were employed to study the microscopic surface morphology of the machined surfaces.

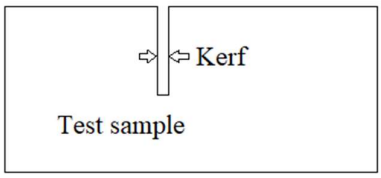

Figure 3 Scheme of measurement of kerf width using optical microscope.

3. Results and discussion

3.1 Effects of T_{on}, T_{off}, and peak current on kerf width

Table 5 presents the kerf width results for the various process parameter settings used during the experiments. Figure 4 shows the influence of the individual control parameters on kerf width. Figure 4(A) reveals that with an increase of current from 2 A to 6 A, kerf width increases by 9.34%. As current is increased there is increase in spark discharge energy [33,34] leading to increase in material vaporization and melting, thus resulting in higher kerf width during machining. With change in current from 2 A to 4 A there is increase in erf width by 2.80%, but from 4 A to 6 A it is observed that kerf width gets increased by 6.36%. In similar studies, but using brass wire electrodes, a linear increase in kerf width has been observed with increase in current up to 6 A [35], but it decreased above 10 A [29]. At current settings greater than 170 A, a similar change in tendency of kerf width was observed at 190 A, above which the kerf width remained constant until 210 A [30]. Therefore, a lower current is suitable to achieve the minimum kerf width, which is consistent with the relationship of current with spark discharge energy.

Figure 4B shows the effect of T_{on} on kerf width. With increase in T_{on} from 20 µs to 50 µs kerf width increases by 12.62%. Further increase in T_{on} from 20 µs to 35 µs has resulted in increase in kerf width by 9.7% but increasing it from 35 µs to 50 µs has resulted in slight increase by 2.65%. With increase in T_{on}, spark intensity and discharge energy increases resulting in increase in rate of material evaporation thus increase kerf width. But beyond this, there is a saturation in the increase of kerf width because, there is not enough time for the melted material to flow away from the machining region, which takes place during duration of T_{off}. Similar to current, lesser durations of T_{on} results in minimum kerf width. A comparable quasi-linear increase in kerf width with T_{on} has been observed in studies involving brass electrodes, for T_{on} between 2 µs - 13 µs [29,35-36] and 100 µs - 120 µs [17,30].

Figure 4C shows the effects of T_{off} on kerf width. Here, there is an initial rise of kerf width by 4.59% from 10 µs to 20 µs. However, further increase in T_{off} from 20 µs to 30 µs results in a drop in kerf width. This is due to the fact that, with increase in duration of T_{off}, there is a better circulation of the dielectric fluid media which flushes out the molten material leading to a much lesser molten zone where material removal takes place. Studies which have considered T_{off} durations in the range of 30 µs - 60 µs have noted an almost linear increase in kerf width with T_{off} [17,30,35]. As per the best knowledge of the authors, only [36] investigated the effect of T_{off} with a partially coinciding range of 10 µs - 14 µs, and their results showed an increase in kerf width with T_{off} which is in consonance with the present study. With a broader range of investigation of 10 µs - 30 µs, the present study revealed that duration of T_{off} closer to 30 µs is better to achieve the minimum kerf width.

Table 5 Quality characteristics obtained from computations at different levels of control parameters.

Serial No.	Current (A)	T_{on} (µs)	T_{off} (µs)	Kerf width (mm)
1	2	20	20	0.100
2	4	35	20	0.112
3	2	50	20	0.115
4	6	35	10	0.123
5	4	20	30	0.098
6	6	20	20	0.113
7	4	50	30	0.117
8	2	35	30	0.105
9	4	5	20	0.118
10	6	50	20	0.123
11	4	35	20	0.117
12	2	35	10	0.107
13	6	35	30	0.108
14	4	50	10	0.108
15	4	20	10	0.098

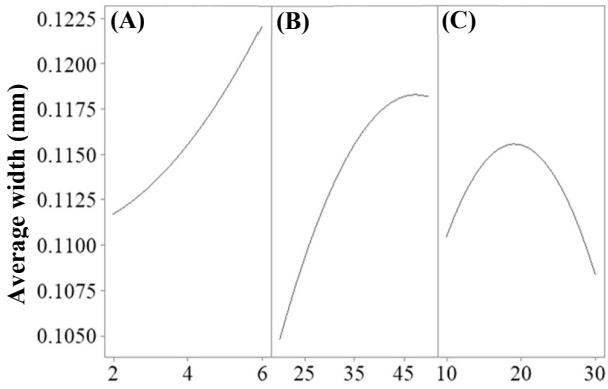

Figure 4 The effect of control factors, (A) Current, (B) T_{on} and (C) T_{off} on kerf width.

3.2 ANOVA of kerf width

ANOVA is carried out on the experimental results obtained from machining at 95% confidence level to evaluate the significance T_{on}, T_{off} and current may have on kerf width. Table 6 lists the results of ANOVA showing the influence of the chosen control factors on kerf width. From the standard Fisher's table, F critical value is found to be 3.29 (for error degree of freedom (DoF) – 3). If the F-value for an input parameter is greater than the critical F-value, it indicates that it has a significant influence on the output. From the table it is seen that, the individual effects of current and T_{on} have significant influence on the kerf width obtained, whereas T_{off} has a non-significant impact. This is consistent with the results obtained using brass electrodes [30]. In case of interaction effects, the interaction between T_{off} and T_{off} is found to be significant on the kerf width, whereas the interaction effects between other control parameters is found to be having no significant influence on the kerf width. A recent study using brass wire electrode also found the interaction effect between T_{off} and T_{off} to be significant, but unlike the present study, the interaction between T_{on} and T_{off} was also found to be significant [36]. This difference in the results could be attributed to the shorter range of T_{off} (10 µs – 14 µs) selected in [36]. In view of minimizing the kerf width, it is advised to keep T_{off} close to 30 µs.

Table 6 ANOVA of kerf width.

Source	DoF	Adjusted sum of squares	Adjusted mean square	F-Value
Current	1	0.000217	0.000217	10.44
Ton	1	0.000356	0.000356	17.10
Toff	1	0.000009	0.000009	0.42
Current*Current	1	0.000007	0.000007	0.34
Ton*Ton	1	0.000060	0.000060	2.88
Toff*Toff	1	0.000138	0.000138	6.63
Current*Ton	1	0.000006	0.000006	0.30
Current*Toff	1	0.000044	0.000044	2.14
Ton*Toff	1	0.000017	0.000017	0.84
Lack-of-Fit	3	0.000080	0.000027	2.21

3.3 Analysis of interaction effects by response surfaces

The interaction effects of T_{on} × current, T_{off} × current, T_{on} × T_{off} on kerf width is shown through the surface plots (Figure 5A-C), respectively. Figure 5A shows that while both T_{on} and current cause an increase in kerf width with their increase, T_{on} has a larger influence on it. The minimum kerf width is achieved at minimum settings of both T_{on} (20 µs) and current 2 A. It is observed from Figure 5(B) that kerf width is increased with the value of current, whereas T_{off} has a contradictory effect, as also seen in Figure 3. At any constant settings of T_{off}, kerf width decreases by decreasing the current. Figure 5(C) shows that the minimum kerf width is obtained at the minimum value of T_{on} (20 µs) and the maximum value of T_{off} (30 µs). This positive relationship between kerf width and T_{on} and the negative relationship between kerf width and T_{off} has also been noted in studies using the ranges: 100 µs ≤ T_{on} ≤ 120 µs, 40 µs ≤ T_{off} ≤ 60 µs [17] and 2 µs ≤ T_{on} ≤ 6 µs, 10 µs ≤ T_{off} ≤ 14 µs [36]. The ANOVA (Table 6) demonstrated that, among the three interaction effects considered, current and T_{off} have the maximum significance, followed by T_{on} and T_{off}, and current and T_{on}. This is validated by the response surfaces, which also show the same order of significance of interaction effects between these control parameters.

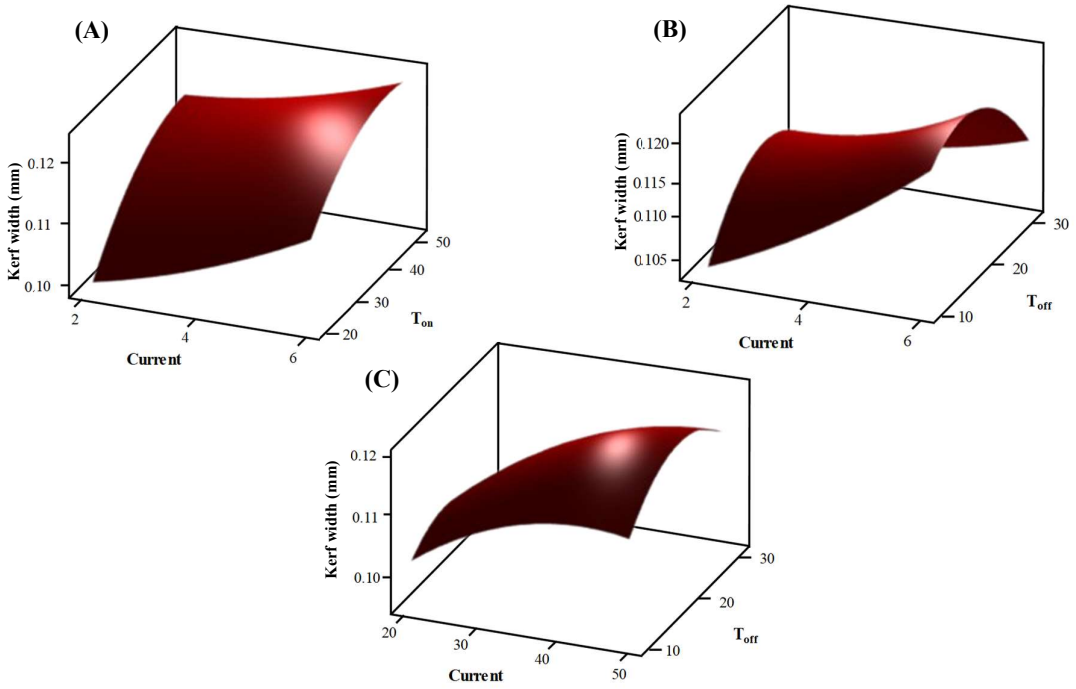

Figure 5 The interaction effects of (A) Current and T_{on}, (B) Current and T_{off} and (C) T_{on} and T_{off} on kerf width (mm).

3.4 Optimization of kerf width

RSM is used for the optimization and Figure 6 shows the optimization plot obtained for kerf width. The figure shows that, the kerf width increases with increase in current. The minimum kerf width is seen at settings of 2 A current. Also, the kerf width increases with duration of T_{on} and minimum kerf width is achieved at 20 µs. Further, the minimum kerf width is obtained at T_{off} duration of 10 µs. Hence, these settings, i.e., current – 2 A, T_{on} – 20 µs, T_{off} – 10 µs are the optimized settings to machine the Ti-6Al-4V alloy by Concord Computer Numerical Control (CNC) Wire-Electrical Discharge Machine (EDM) machine using molybdenum electrode to achieve the minimum kerf width. The estimated kerf width at these optimized conditions is 0.0935 mm. Confirmation experiments were carried out at these settings to validate this finding, and the results are shown in Table 7.

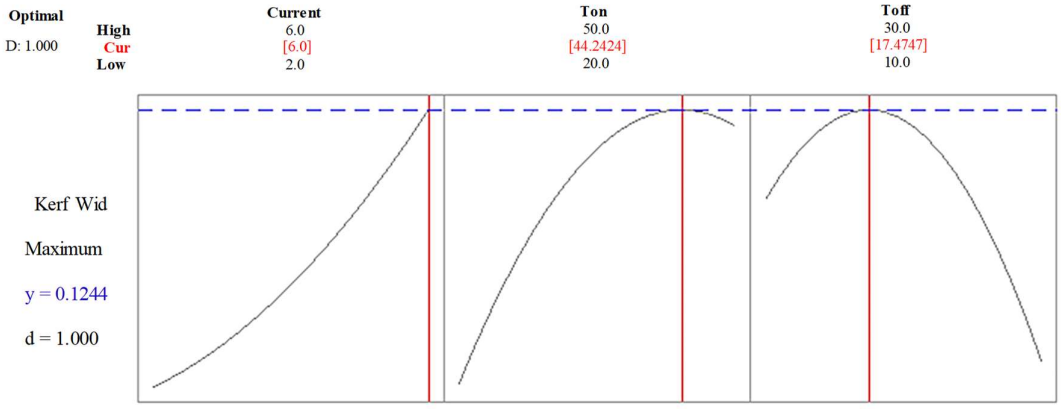

Figure 6 The effect of current, T_{on} and T_{off} on kerf width.

Table 7 Comparison of predicted and experimental kerf width at optimized settings.

Trial No.	Optimized kerf width (mm)	Experimental kerf width (mm)	Error (%)
1		0.087	6.95
2		0.099	5.88
3	0.0935	0.101	8.02
4		0.106	13.37
5		0.095	1.60

3.5 Regression modelling of kerf width with respect to the control parameters

To model a mathematical relationship between the control parameters (Interrupting Capacity (I_c): Current, T_{on}: Pulse-on time, T_{off}: Pulse-off time) with the output parameter in this study, i.e., kerf width, a regression model is developed, given by Equation (1). The coefficient of determination (R^2) for the developed model is 90.11%. Regression models have been developed for kerf width in WEDM of Ti-6Al-4V with respect to current, T_{on} and T_{off} [29-30]. But the range of control settings in these studies are mostly at higher current settings (>8 A). Therefore, our prediction will be suitable for low current settings. The accuracy of the predicting with the experimental data is verified. Table 8 shows the confirmation of the developed model with experimental results under the same operating settings. The model is valid in between the operated range: 2 A ≥ I_c ≤ 6 A, 20 µs ≥ T_{on} ≤ 50 µs, 10 µs ≥ T_{off} ≤ 30 µs.

$$\begin{aligned}\text{Kerf width} = {} & 0.0414 + 0.00462I_c + 0.001586T_{on} + 0.00252T_{off} + 0.000347I_c^2 \\ & - 0.000018T_{on}^2 - 0.000061T_{off}^2 - 0.000042I_c \times T_{on} - 0.000167I_c \times T_{off} \\ & + 0.000014T_{on} \times T_{off}\end{aligned} \quad (1)$$

Table 8 Comparison of predicted and experimental kerf width using the developed regression model.

Trial No.	I_c (A)	T_{on} (µs)	T_{off} (µs)	Predicted (mm)	Experimental (mm)	Error (%)
1	2	20	10	0.093	0.099	5.96
2	3	25	15	0.105	0.112	6.22
3	4	35	20	0.115	0.122	5.67
4	5	45	25	0.118	0.132	11.49
5	6	50	30	0.115	0.126	9.61
6	2	10	30	0.082	0.077	6.56

Figure 7(A-D) presents the results of the residual analysis for the regression model which is developed to predict the kerf width. The probability plot (Figure 7A) highlights that except a few small outliers, most of the residuals are spread around a line of fit indicating a reasonable correlation of the model. The plot of residuals with respected to the fitted values Figure 7B shows that the residuals are arbitrarily distributed around the mean which suggests the unbiasedness of the results obtained from the model [36]. The histogram of the residuals of kerf width is presented in Figure 7(C) Finally, the residuals obtained at several experimental trials is presented in Figure 7(D) which shows a similar random scattering of the results, implying the applicability of the results over the entire range of the control parameter values [36]. The developed regression model is therefore aligned with the basic conditions required in linear regression analyses, i.e., linearity, homoscedasticity, and normality.

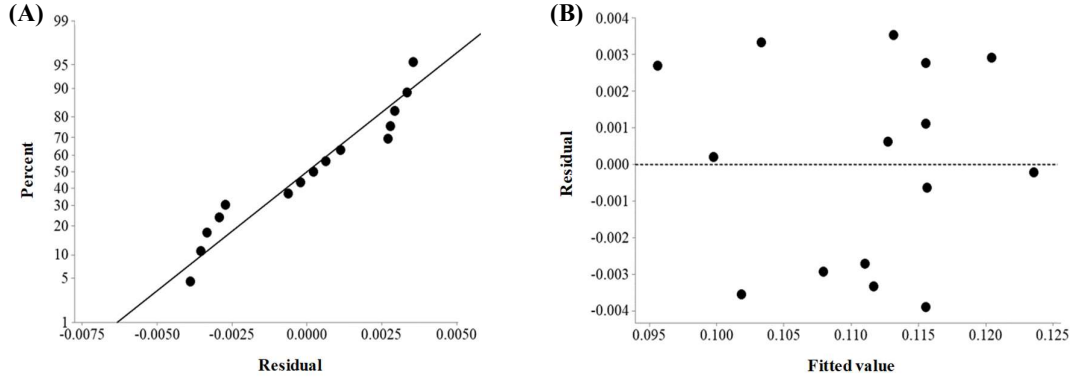

Figure 7 Distribution of residuals with (A) normal probability plot and (B) versus fit plot.

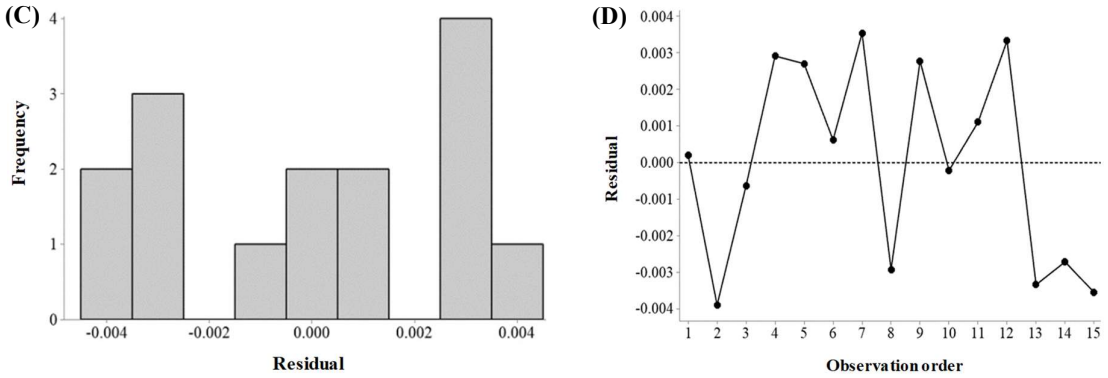

Figure 7 (continued) Distribution of residuals with (C) histogram and (D) versus order plot.

3.6 Analysis of the machined surface micrographic morphology

Scanning electron microscopy (SEM) is utilized to carry out surface characterization of the machined titanium alloy. The machined surface (Figure 8A). shows the formation of ridges and microcracks at 1000X magnification [37]. Figure 8(B) shows the presence of cracks which usually developed because of the rapid cooling of the pool of molten metal during the period of deionization due to the flow of dielectric fluid medium. Additionally, a layered recast formation is presented due to the solidification of the molten metal. At 3000X magnification (Figure 8C), the voids (average size around 22 µm) are found among the surface layers [38,40]. Further morphological study at magnification of 3000X. Figure 8D showed the existence of globules identified along the machined surface. Globules are typically formed from the solidification of molten metal when exposed to dielectric fluid medium (deionized water in the present study) [41].

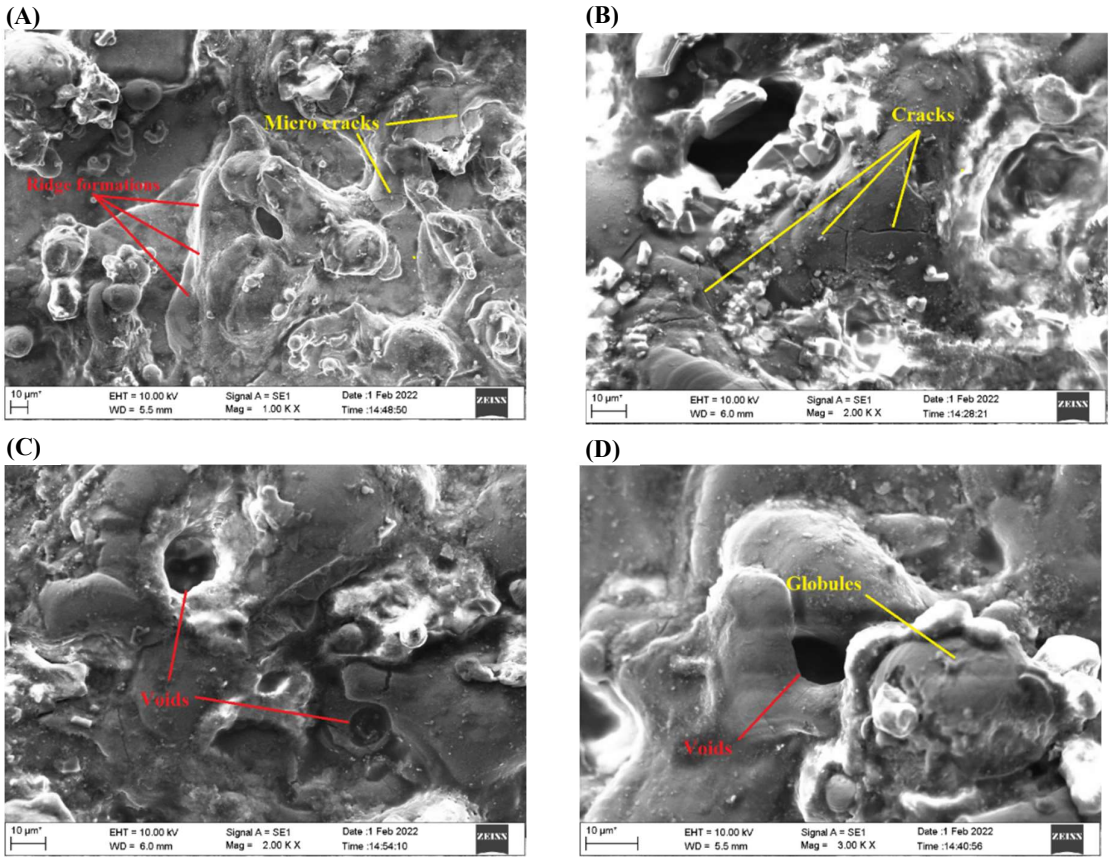

Figure 8 SEM images of the machined surface showing (A) void and crack formations at 1000X, (B) crack formation at 2000X, (C) voids at 2000X and (D) void and globule formations at 3000X magnification.

4. Conclusion

In the present study, the effects of peak current, T_{on}, and T_{off} on kerf width is investigated in Wire-Electric Discharge (WED) machining of Ti-6Al-4V. Series of experiments were conducted using 0.18 mm molybdenum wire as electode and deionized water as dielectric fluid. The results are useful for predicting the kerf width and choosing the optimum process parameter settings for machining of Titanium alloy Ti-6Al-4V in WEDM industry.The following conclusions have been drawn from this work:Increase in peak current from 2 A to 6 A and T_{on} from 20 µs to 50 µs increases the kerf width by 9.34% and 12.62%, respectively. Increase in T_{off} from 20 µs to 30 µs caused a sharp reduction in kerf width. ANOVA of kerf width indicated that the individual effects of current and T_{on} have significant impact on the kerf width, whereas that of T_{off} is not significant. However, in case of interaction effects, the second-order effect of T_{off} on T_{off} is found to be significant whereas other interaction effects are statistically insignificant. ANOVA in conjunction with interaction effect response surfaces showed that interaction effects between the different parameters can be ranked in the order of significance of influence as: current and T_{off} - I, T_{on} and T_{off} - II and current and T_{on} - III. RSM optimization showed that current - 2 A, T_{on} - 20 µs, T_{off} - 10 µs are the optimized control settings to machine the Ti-6Al-4V alloy by Concord CNC WEDM machine using molybdenum electrode to achieve the minimum kerf width. Morphological study of machined cut surfaces showed the presence of recast layers on which microcracks were present. Furthermore, the presence of globules, wavy formations, ridge and crater formations and voids were revealed at the microscopic level. The developed regression model predicts the kerf width with an R^2=90.11%, valid in the control parameter range: 2 A $\geq I_c \leq$ 6 A, 20 µs $\geq T_{on} \leq$ 50 µs, 10 µs $\geq T_{off} \leq$ 30. At the optimum control parameter settings (I_c - 2 A, T_{on} - 20 µs, T_{off} - 10 µs) the correspondingly minimized Kerf width obtained is 0.0935 mm.

5. Acknowledgements

The authors express their sincere appreciativeness to Manipal Institute of Technology, Manipal Academy of Higher Education, Manipal, India, for providing the required infrastructural facilities and encouragement to carry out this research project.

6. References

[1] Pramanik A, Littlefair G. Machining of titanium alloy (Ti-6Al-4V) - theory to application. Mach Sci Technol. 2015;19(1):1-49.
[2] Gupta K, Laubscher R. Sustainable machining of titanium alloys: a critical review. Proc Inst Mech Eng Part B J Eng Manuf. 2016;231(14):2543-2560.
[3] Pramanik A. Problems and solutions in machining of titanium alloys. Int J Adv Manuf Technol. 2014;70: 919-928.
[4] Oke SR, Ogunwande GS, Onifade M, Aikulola E, Adewale ED, Olawale OE, et al. An overview of conventional and non-conventional techniques for machining of titanium alloys. Manuf Rev. 2020;7:34.
[5] Nishanth BS, Kulkarni VN, Gaitonde VN. A review on conventional and nonconventional machining of titanium and nickel-based alloys. AIP Conf Proc. 2019;2200(1):020091.
[6] Astakhov VP. Ecological machining: near-dry machining. In: Davim JP editor. Machining: fundamentals and recent advances. 1st ed. London: Springer; 2008. p. 195-223.
[7] Davim JP. Nontraditional machining processes. 1st ed. London: Springer; 2013.
[8] Davim JP. Machining of titanium alloys. 1st ed. Heidelberg: Springer; 2014.
[9] Qudeiri JAE, Mourad AHI, Ziout A. Electric discharge machining of titanium and its alloys: review. Int J Adv Manuf Technol. 2018;96:1319-1339.
[10] Hourmand M, Sarhan AAD, Sayuti M, Hamdi M. A Comprehensive review on aachining of titanium alloys. Arab J Sci Eng. 2021;46**:**7087-7123.
[11] Festas A, Ramos A, Davim JP. Machining of titanium alloys for medical application - a review. Proc Inst Mech Eng, Part B: J Eng Manuf. 2021;236(4):309-318.
[12] Saedon JB, Jaafar N, Yahaya MA, Saad N, Kasim MS. Multi-objective Optimization of titanium alloy through orthogonal array and grey relational analysis in WEDM. Proc Technol. 2014;15:832-840.
[13] Raj SON, Prabhu S. Modeling and analysis of titanium alloy in wire cut EDM using grey relation coupled with principle component analysis. Aust J Mech Eng. 2017;15(3):198-209.
[14] Mohamed MF, Lenin K. Optimization of wire EDM process parameters using Taguchi technique. Mater Today: Proc. 2020;21:527-530.
[15] Nourbakhsh F, Rajurkar KP, Malshe AP, Cao J. Wire electro-discharge machining of titanium alloy. Procedia CIRP. 2013;5:13-18.

[16] Golshan A, Ghodsiyeh D, Izman S. Multi-objective optimization of wire electrical discharge machining process using evolutionary computation method: effect of cutting variation. Proc Inst Mech Eng, Part B: J Eng Manuf. 2015;229(1):75-85.
[17] Arikatla SP, Mannan KT, Krishnaiah A. Parametric optimization in wire electrical discharge machining of titanium alloy using response surface methodology. Mater Today Proc. 2017;4(2):1434-1441.
[18] Chaudhari R, Vora J, Parikh DM, Wankhede V, Khanna S. Multi-response Optimization of WEDM parameters using an integrated approach of RSM-GRA analysis for pure titanium. J Inst Eng (India): D. 2020;101(1):117-126.
[19] Fuse K, Dalsaniya A, Modi D, Vora J, Pimenov DY, Giasin, K, et al. Integration of fuzzy AHP and fuzzy TOPSIS methods for wire electric discharge machining of titanium (Ti6Al4V) alloy using RSM. Materials. 2021;14(23):7408.
[20] Khanna, N, Davim JP. Design-of-experiments application in machining titanium alloys for aerospace structural components. Meas. 2015;61:280-290.
[21] Lauro CH, Filho SLMR, Brandao LC, Davim JP. Analysis of behaviour biocompatible titanium alloy (Ti-6Al-7Nb) in the micro-cutting. Meas. 2016;93:529-540.
[22] Hascalik A, Caydas U. Electrical discharge machining of titanium alloy (Ti-6Al-4V), Appl Surf Sci. 2007;253(22):9007-9016.
[23] Sivakumar K, Gandhinathan R. Establishing optimum process parameters for machining titanium alloys (Ti6Al4V) in spark electric discharge machining. Int J Eng Adv Technol, 2013;2:201-204.
[24] Uthirapathi A, Singaravelu DL. Effect of rotating tool electrode on machining of titanium alloy using electric discharge machining. Adv Mater Res. 2013;651:448-452.
[25] Chaudhari R, Vora JJ, Patel V, Lacalle LNLd, Parikh DM. Effect of WEDM process parameters on surface morphology of nitinol shape memory alloy. Materials. 2020;13(21):4943.
[26] Devarasiddappa D, Chandrasekaran M, Arunachalam R. Experimental investigation and parametric optimization for minimizing surface roughness during WEDM of Ti6Al4V alloy using modified TLBO algorithm. J Braz Soc Mech Sci Eng. 2020;42:128.
[27] Chakraborty S, Mitra S, Bose D. Performance analysis on eco-friendly machining of Ti6Al4V using powder mixed with different dielectrics in WEDM. Int J Automot Mech Eng. 2020;17(2):8128-8139.
[28] Sivaprakasam P, Hariharan P, Gowri S. Modeling and analysis of micro-WEDM process of titanium alloy (Ti-6Al-4V) using response surface approach. Eng Sci Technol Int J. 2014;17(4):227-235.
[29] Sneha P, Mahamani A, Kakaravada I. Optimization of wire electric discharge machining parameters in machining of Ti-6Al-4V Alloy. Mater Today Proc. 2018;5(2):6722-6727.
[30] Sonawane SA, Ronge BP, Pawar PM. Multi-characteristic optimization of WEDM for Ti-6Al-4V by applying grey relational investigation during profile machining. J Mech Eng Sci. 2019;13(4):6059–6087.
[31] Doreswamy D, Javeri J. Effect of process parameters in EDM of D2 steel and estimation of coefficient for predicting surface roughness. Int J Mach Mach Mater. 2018;20:101-117.
[32] Deepak D, Shrinivas P, Hemant G, Iasy R. Optimisation of current and pulse duration in electric discharge drilling of D2 steel using graphite electrode. Int J Automot Mech Eng. 2018;15:5914-5926.
[33] Lenin N, Sivakumar M, Selvakumar G, Rajamani D, Sivalingam V, Gupta, M, et al. Optimization of process control parameters for WEDM of Al-LM25/Fly Ash/B4C hybrid composites using evolutionary algorithms: a comparative study. Metals. 2021;11:1105.
[34] Aggarwal V, Pruncu CI, Singh J, Sharma S, Pimenov DY. Empirical investigations during WEDM of Ni-27Cu-3.15Al-2Fe-1.5Mn based superalloy for high temperature corrosion resistance applications. Materials. 2020;13:3470.
[35] Rao KV, Raju LR, Kumar CK. Modeling of kerf width and surface roughness in wire cut electric discharge machining of Ti-6Al-4V. Proc Inst Mech Eng E: J Process Mech Eng. 2020;234(6):533-542.
[36] Abebe T, Palani S, Prakash JU. Kerf width analysis of wire electrical discharge machining of titanium alloy (Ti-6Al-4 V ELI) using response surface method. Mater Today Proc. 2022;62(2):481-487.
[37] Chiang KT, Chang FP, Tsai DC. Modeling and analysis of the rapidly resolidified layer of SG cast iron in the EDM process through the response surface methodology. J Mater Proc Technol. 2007;182(3):525-533.
[38] Li L, Guo YB, Wei XT, Li W. Surface integrity characteristics in Wire-EDM of Inconel 718 at different discharge energy. Procedia CIRP. 2013;6:220-225.
[39] Xu B, Lian MQ, Chen SG. Combining PMEDM with the tool electrode sloshing to reduce recast layer of titanium alloy generated from EDM. Int J Adv Manuf Technol. 2021;117:1535-1545.
[40] Sahu A, Mahapatra SS. Surface characteristics of EDMed titanium alloy and AISI 1040 steel workpieces using rapid tool electrode. Arab J Sci Eng. 2020;45:699-718.
[41] Arooj S, Shah M, Sadiq S. Effect of current in the EDM machining of aluminum 6061 T6 and its effect on the surface morphology. Arab J Sci Eng. 2014;39:4187-4199.